Forestry An International Journal of Forest Research

Institute of Chartered Foresters

Forestry 2023; **96**, 672–689, https://doi.org/10.1093/forestry/cpad002
Advance Access publication 31 January 2023

Aboveground responses to belowground root damage detected by non-destructive sensing metrics in three tree species

Matan Azar[1], Gabriel Mulero[2], Yaara Oppenheimer-Shaanan[1], David Helman[2,3] and Tamir Klein[1,*]

[1]*Department of Plant and Environmental Sciences, Weizmann Institute of Science, Rehovot 7610001, Israel*
[2]*Department of Soil and Water Sciences, Institute of Environmental Sciences, The Robert H. Smith Faculty of Agriculture, Food and Environment, The Hebrew University of Jerusalem, Rehovot 7610001, Israel*
[3]*The Advanced School for Environmental Studies, The Hebrew University of Jerusalem, Jerusalem 9190401, Israel*

*Corresponding author. Tel: +972-8-934-3505; E-mail: tamir.klein@weizmann.ac.il

Received 24 April 2022

Root systems form a significant part of tree biomass and function. Yet, roots are hidden from our eyes, making it difficult to track the belowground processes. By contrast, our capacity to detect aboveground changes in trees has been continuously improving using optical methods. Here, we tested two fundamental questions: (1) To what extent can we detect aboveground responses to mechanical damage of the root system? (2) To what extent are roots redundant? We applied three different non-destructive remote sensing means: (1) optical means to derive leaf greenness, (2) infrared means to detect the changes in leaf surface temperature and (3) spectral means to derive five vegetation indices (i.e. the photochemical reflectance index (PRI), the chlorophyll photosynthesis index ($CI_{Red\text{-}edge}$), the anthocyanin reflectance index 1, the structure insensitive pigment index and the normalized difference water index (NDWI)). We recorded the above metrics for hours and days and up to a month following induced root damage in three key Mediterranean tree species: Aleppo pine (*Pinus halepensis* Mill.), Palestine oak (*Quercus calliprinos* Webb.) and Carob (*Ceratonia siliqua* L.). To induce root damage, we removed 25, 50 and 75 percent of the root system in each species and compared it with control saplings. Tree aboveground (canopy) responses to root damage increased over time and with damage level. Leaf warming (up to 3°C) and decreased PRI were the most significant and rapid responses, with temperature differences being visible as early as 2 days following root damage. NDWI and greenness were the least sensitive, with responses detectable only at 75 percent root damage and as late as 14 or 30 days following root damage. Responses varied vastly among species, with carob being the most sensitive and pine being the least. Changes in leaf temperature and PRI indicated that leaf transpiration and photosynthesis were impaired by root damage. Although trees build roots in excess, mechanical damage will eventually decrease transpiration and photosynthesis across tree species.

Introduction

Root systems of trees usually account for 20–50 percent of their biomass (Crowther *et al*., 2019). Yet, our knowledge of tree life is heavily biased towards studying aboveground parts. As soil is typically a dense and opaque media, we need to expose the roots via excavation to examine them. However, exposing the root system disturbs its native environment, thus altering its structure and functioning. This is why root health is very difficult to assess in the field. In analogy to leaves, roots are assumed to be produced by plants in excess, that is plants produce more roots than required to maintain an adequate tree functioning (Sachs and Novoplansky, 1993; Zhang and Zhang, 2000; Ma *et al*., 2018). Thus, a fundamental question concerns the minimal root fraction a tree needs. In turn, we could also ask whether belowground root damage—leading to a reduction of functioning root fraction—could be detected aboveground by non-destructive sensing metrics. This question has broad implications for forest management (Rog *et al*., 2021), urban landscaping (Čermak et al. 2013), orchard management and various land-use change scenarios. Evidently, root damage can result from various processes, e.g.: (1) strong winds that do not cause uprooting but still damage roots, (2) drought that leads to fine root mortality, (3) chemical or biotic attack on roots and (4) mechanical damage to roots from the use of heavy machinery in forestry, either directly or indirectly due to soil compaction.

The topic of aboveground–belowground interactions is a growing study area (Bardgett, 2018). In contrast to root systems, the aboveground parts of trees are easy to observe and often form the landscape. For example, in apple trees attacked by a pest beetle feeding on roots, herbivore-induced plant volatiles and plant–plant communication were measured below- and aboveground (Abraham *et al*., 2015). Belowground organisms can induce defence responses to aboveground damage and vice

versa (Bezemer and van Dam, 2005). Similarly, belowground chemical damage to the root system can translate into phenotypic differences aboveground. In a *Picea abies* plot in Slovakia exposed to acid deposition, it was found that annual fine root production decreased with increasing phenotypic crown stress (Konopka and Lukac, 2010).

Among damage scenarios, it seems that physical (mechanical) damage has not been studied as thoroughly as chemical damage, and more so, biological damage. However, trees are often exposed to mechanical damage, for example, by storms and human activities. Among four tropical rainforest tree species, effects of induced aboveground mechanical damage like crown loss, stem breakage and stem pinning by fallen debris revealed interspecific differences in post-damage vegetative recovery and survival (Guariguata, 1998). Belowground damage has been studied as well. For example, root pruning is a general practice in gardening and landscaping. The effects on growth, photosynthesis and leaf minerals were primarily expressed following repetitive root pruning or in the subsequent dry season (Schupp and Ferree, 1988, Benson *et al.*, 2019). In mature urban trees (*Celtis occidentalis* and *Fraxinus pennsylvanica*), both aboveground damages (defoliation and stem injuries) and belowground (37 and 75 percent root reduction) damages were examined. Root injury was the most impactful treatment for *Celtis*, consistently decreasing root and stem growth throughout the 5 years following the treatment. By contrast, defoliation decreased growth only in the first 2 years (Vitali *et al.*, 2019). Low-intensity stress-triggered compensatory reactions stimulate photosynthetic rates and nutrient utilization. The slower-growing tree species, *Celtis*, showed a less adverse reaction to all damage treatments compared with *Fraxinus* (Vitali *et al.*, 2019). Lastly, root severance by trenching around young urban trees (*Aesculus hippocastanum* and *Tilia* × *europea*) showed that growth reduction was associated with mild water stress and photoinhibition (Fini *et al.*, 2013). Damage effects on trees developed over time, peaking at 2 months after trenching.

Since roots are the major source of water and nutrient uptake, belowground damage should directly affect the water and nutrient supply to stems and leaves. When the ratio between leaf area and root area increases abruptly, a demand–supply imbalance develops. In turn, these effects can translate into phenotypic responses such as leaf desiccation, discoloration and ultimately leaf shedding. Dror *et al.* (2020) examined how mature olive trees responded to breakage of the root-soil connection, followed by transplanting at a nearby site. Among several functional parameters measured over months and years, leaf photosynthesis and transpiration showed the most significant and consistent reductions, up to 60 per cent.

Recent developments in optical and remote sensing methods pave the path to new opportunities in studying tree ecophysiology. These remote sensing methods span from using satellites to detect forest canopy height (Klein *et al.*, 2015), forest health (Helman *et al.*, 2017b) and forest drought vulnerability (Helman *et al.*, 2017a) to using handheld cameras to study the dynamics in leaf greenness (Winters *et al.*, 2018) and temperature in trees (Lapidot *et al.*, 2019) and crops (Mulero *et al.*, 2022). Spectral-based vegetation indices, such as the photochemical reflectance index (PRI) and the normalized difference water index (NDWI), have been used to track changes in the photosynthesis activity (Filella *et al.*, 2004; Garbulsky *et al.*, 2011; Peñuelas *et al.*, 2011; Zhang *et al.*, 2017) and plant water status (Helman and Mussery, 2020). For example, PRI demonstrated sensitivity to diurnal changes in the physiological indicators of water stress in an olive orchard with diurnal airborne imagery (Suárez *et al.*, 2008). In maize and sorghum, PRI and canopy temperature were more useful in detecting the leaf fluorescence yield changes caused by water stress than sun-induced chlorophyll fluorescence (Panigada *et al.*, 2014). Still, the utility of these indices has not yet been tested in relation to root damage.

Here, we set out to test the following research questions: (1) To what extent can aboveground responses to belowground mechanical damage be detected through non-destructive thermal and spectral sensing? Once detected, (2) What is the rate of aboveground response of each metric to belowground damage? (3) What is the minimum root system fraction required to maintain tree survival? We hypothesized that root damage would induce a fast reduction (hours to a few days) in tree water uptake, expressed in leaf warming and desiccation. On the other hand, we assumed that the feedback on photosynthesis will be slower (several days), eventually reducing leaf greenness (days to weeks) and impacting the other spectral-based vegetation indices. Based on a few previous studies on the topic (Fini *et al.*, 2013; Benson *et al.*, 2019; Vitali *et al.*, 2019; Dror *et al.*, 2020), we hypothesized that the above responses would appear at high root damage (e.g. ≥50 percent), but not at low root damage (e.g. 25 percent), due to root redundancy. To test our hypothesis, we removed 0, 25, 50 and 75 percent of the root systems of 2.5-year-old saplings of three key Mediterranean forest tree species and followed their phenotypic responses using three non-destructive means: RGB, infrared (IR) and near-IR spectral imageries. For the sake of simplicity, we mechanically reduced the root biomass by cutting roots. We hypothesize that the related root loss could result from any inducer, be it physical, chemical or biological. After inducing the damage, images were used to track the leaf greenness, leaf temperature, radiation use efficiency (RUE; measured by PRI), photosynthesis (measured by $CI_{Red\text{-}edge}$ and structure insensitive pigment index (SIPI)), anthocyanin content (measured by anthocyanin reflectance index 1 (ARI1)) and water stress (measured by NDWI).

Materials and methods

Plant material and conditions

Our study was conducted on 2.5-year-old saplings growing in a net house at the Weizmann Institute of Science (Rehovot, Israel). Climate is warm Mediterranean, and weather conditions during the experiment (November 2020) were typical of the autumn season at the site, with minimum and maximum diurnal temperatures of 9.4°C and 20.1°C, mild wind (0–3 m s^{-1}) and with a few rain events, totalling ∼70 mm. Our study species were common forest tree species from the Mediterranean forest and maquis: (1) Aleppo pine (*Pinus halepensis* Mill.), a coniferous species occurring across a wide range of sites in the Mediterranean basin. The tree is evergreen, reaches 20–30 m and is drought resistant. The leaves are needle-shaped and paired to one called brachiblast. (2) Palestine oak (*Quercus calliprinos* Webb.), an evergreen broadleaf,

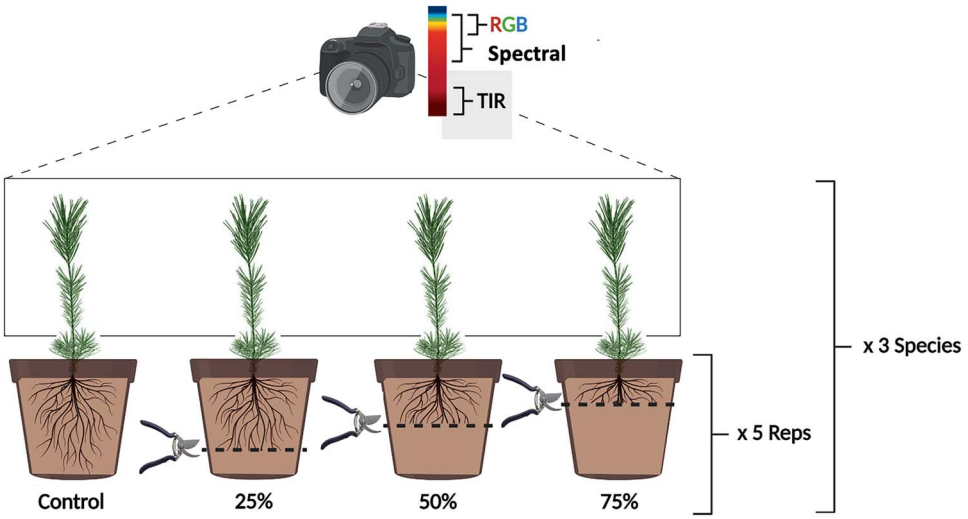

Figure 1 A scheme of the experimental layout: root systems of five saplings of each of three tree species were pruned to three different levels (and an unpruned control). Canopy responses were monitored along hours and days and up to a month using three non-destructive remote sensing means: optical (red, green, blue (RGB)) TIR and spectral means.

the most common tree in the Israel maquis. It reaches up to 15 m in height, and its trunk diameter reaches up to 2 m. The leaves are small, stiff and dentate, changing their shape in the phase transition from juvenility to maturity. (3) Carob (*Ceratonia siliqua* L.) is a dioecious broadleaf evergreen tree that lives in the wild as well as cultivated in Israel and throughout the Mediterranean. The tree reaches up to 10 m with a thick trunk and the leaves are fresh green and pennate.

Experimental setup

The 2.5-year-old saplings were 0.8–1.2 m tall. They originated from seeds collected in the Jerusalem Mountains, Israel, and were sprouted by the Jewish National Fund (JNF) Forest service nursery from February to April 2017. Seedlings were transferred to plastic 'quick-pots 585' (200-mL plugs, 5 × 5 cm) in the Eshtaol nursery (JNF). At the Weizmann Institute, all seedlings were transplanted to 10-L pots. To avoid shock and enable the root system to develop, saplings were grown under a sustained irrigation regime (60 mL, three times a day) without fertilization. They received a natural light regime in a glasshouse until the transfer to the net-house. Saplings were arranged in an area of 15 × 5 m in the middle of the net-house (30 × 20 m). The net-house was devoid of any climate control, and hence, saplings were exposed to the native conditions (above). All pots contained natural forest soil mixed with washed sand and tuff (5/10/1 v/v). During the experiment, saplings were drip irrigated with 30 mL for three times a day (90 mL day^{-1}). The planting soil was not fertilized, and the saplings were not sprayed. Twenty plants from each species were divided into four treatments, representing 0, 25, 50 and 75 percent removal of the root system (Figure 1). The cylindrical pots were first marked with lines at 0, 25, 50 and 75 percent of pot height (bottom to top) and were then sawed along the lines. Saplings that were not sawed (0 percent) were used as controls. To ensure that all pots are simultaneously sawed, eight helpers were recruited to expedite the preparation of treatments. All saplings were put back to their pots for the rest of the experiment. We left some free soil at the bottom of each pot (otherwise, pots were too light and tipped over). Six months following the end of the experiment, we detected new root growth into the soil at the bottom of each pot across treatments and species. Each sapling was marked with its treatment level (either 0, 25, 50 or 75 percent root system removed) and replicate label (A–E). For each photograph, four saplings of the same species and marked with the same letter, i.e. representing each of the treatments, were arranged in front of a black velvet screen. The cameras were placed in a fixed position 1.2 m from the row of four saplings, at 90° to the row. Due to sapling morphology, self-shading in the foliage was rather low across the species, aiding the selection of sunlit leaves for image analysis. Due to the differences in instrument and expert availability, not all parameters were measured at all times. Image capture and analysis are detailed below. Still, each parameter was measured at early (3 h–4 days) and late (14–30 days) time-points following root cutting. The original plan included additional sensing metrics, namely estimates of leaf elements using an X-ray fluorescence machine and measurements of free-air volatile organic compounds emissions. However, since preliminary results were inconsistent for unknown reasons, these measurements were discontinued.

Root system biomass and architecture

Before transfer to the net-house, three saplings from each species were harvested and were sectioned into five major compartments: tap root, lateral roots, branches, stem and leaves. All compartments were dried in an oven (60°C for 48 h), followed by weighing for biomass partitioning. We observed that in all nine saplings, roots reached the bottom of the pot (20 cm). Total biomass was lower for *Ceratonia* (82.1 ± 7.5 g) than for *Quercus* (114.5 ± 11.0 g) and *Pinus* (121.7 ± 22.3 g). Similarly, total root biomass was 23–34 g in *Ceratonia*, 40–58 g in *Pinus*

and 51–74 g in *Quercus*. Despite these differences, biomass was partitioned equally between tap root and lateral roots and across the three species: lateral roots accounted for 49.7 ± 1.3 percent of total root biomass in *Ceratonia*, 50.2 ± 3.9 percent in *Pinus* and 49.2 ± 0.8 percent in *Quercus*.

Leaf greenness

We used a Nikon D7200 camera (Tokyo, Japan), including a Kodak greyscale in the image (for calibration purposes), to photograph the saplings. This RGB camera is an SLR camera equipped with a Toshiba CMOS sensor (23.5 × 15.6 mm), 24.2 Mpixel and 3:2 aspect ratio. The lens is a Nikkor AF-S with focal length of 18–140 mm (technical data taken from the manufacturer). Images were analysed using ImageJ software (github.com/imagej/imagej1), and the Green chromatic coordinate (GCC) index (on a scale of 0–1) was calculated by the equation:

$$\mathrm{GCC} = \frac{\text{Intensity of green channel}}{\text{RGB}\ (\text{Red} + \text{Green} + \text{Blue})}. \quad (1)$$

GCC was calculated for each of nine pixels (3 × 3) manually selected from the centre of sunlit leaf areas of each sapling. These replicates ($n = 10$) were used to produce a mean value per sapling (species, treatment and replicate) and time-point and were not considered in the statistical analysis, where only sapling replicates were considered.

Leaf temperature

We used a thermal infrared (TIR) camera in order to evaluate the changes in leaf temperature. We demonstrated, in a previous experiment, for the three species, that leaf temperature changes could be used as an index for transpiration rate due to evaporative cooling from the leaf surface (Lapidot *et al.*, 2019). The camera was a FLIR T1030sc (FLIR Systems Inc., Wilsonville, OR, USA), with 14-bit, 1027 × 768-pixel resolution, 30 frame rate per second, accuracy of ±1°C or 1 percent of the temperature reading between 5–150°C, 7.5–14 μm spectral range, 24.6 mm focal length, 21° × 28° field of view (FOV) and built-in 5 Mpixel digital camera, adapted to the IR lens (technical data taken from the manufacturer). TIR images were processed using FLIR ResearchIR Max software (FLIR Systems Inc.). Image parameters of relative humidity and air temperature were set for each image. The emissivity was set to a value of 0.98, as recommended by Idso *et al.* (1969). TIR images were saved as eight-bit grey-level TIFF images. Each image was aligned to its matching visual image using the Fiji package for image processing (Schindelin *et al.*, 2012). Both types of images had corresponding pixels and the same dimensions. For each image, 10 regions of interest (ROIs) of 9 pixels (3 × 3) each were manually selected from the centre of the sunlit part of the leaf. This approach was used to avoid observed leaf cooling due to self-shading (Figure 2), exacerbated by our imaging at the side view of the saplings rather than a top view. The ROI was limited to the centre of the leaf to avoid edge effects. $\Delta T_{\text{leaf-air}}$ was calculated as an average of the 10 ROIs per sapling.

Spectral imaging and image processing

We used the SpecimIQ hyperspectral camera (Specim Ltd, Oulu, Finland), which is a push broom portable handheld camera. The SpecimIQ camera is an integrated operating and controls system that enables easy pre-processing and classification within the camera's software (Behmann *et al.*, 2018). It covers the wavelengths within the visible–near-IR range (VIS–NIR = 400 nm—1000 nm), having a total of 204 spectral bands with a 7-nm FWHM bandwidth and a FOV of 0.55 × 0.55 m at 1-m distance and a spatial resolution of 512 × 512 pixels. A 10×10-cm white reference calibration panel (90 percent reflectance) was used in the scene to enable transforming radiance values into relative reflectance. The hyperspectral SpecimIQ camera comes with pre-installed software that allows hyperspectral data capturing and data processing to change the radiance values into relative reflectance and other analytical options (Behmann *et al.*, 2018).

Images were taken with the camera fixed on a tripod ∼3 m away from the saplings for a good FOV of all five-replicate pots of each species at a time. To properly represent illumination conditions, the white reference panel was located next to the sample, and the images were taken using the simultaneous white reference setting of the camera (see Figure 2). The integration time was set depending on the illumination conditions. The plants were placed before a black non-reflective background to minimize light scattering on the plant samples. Since the SpecimIQ software does not support the direct calculation of vegetation indices, reflectance data from the captured images were extracted using Headwall's Hyperspec III software (Headwall Photonics, Fitchburg, MA, USA). We selected the pixels from the mid-even portion of the plant canopy as the ROI. All vegetation indices were calculated from the spectral data per pixel and were then averaged over the ROI for each replicate pot.

Vegetation indices

We used five spectral indices to detect the aboveground responses to belowground damage: the PRI, the chlorophyll photosynthesis index ($\mathrm{CI_{Red\text{-}edge}}$), the SIPI, the ARI1 and the NDWI. Table 1 presents the formulation and sources of the five indices.

PRI has been shown to be a good proxy of RUE (Gamon *et al.*, 1997; Filella *et al.*, 2004; Garbulsky *et al.*, 2011), which is a biophysical parameter that determines the efficiency of the plant to use the absorbed energy in photosynthesis (Monteith, 1977). Plants dissipate excess energy through the de-epoxidation of violaxanthin (xanthophyll pigment) to zeaxanthin, which is reflected in the absorbance of light at the yellow band of the visible spectrum (∼530 nm). Such a dissipation mechanism is related to the RUE of the plant, and the accompanied pigment change is the basis for the PRI calculation (Demmig-Adams and Adams, 2006; Kohzuma *et al.*, 2021; Zhang *et al.*, 2017). PRI and RUE correlations were found at various levels and scales (Gamon *et al.*, 2005; Porcar-Castell *et al.*, 2012; Kováč *et al.*, 2018; Sukhov *et al.*, 2021), and since PRI can be derived from remote sensing, its use opens up a great opportunity for modeling RUE from space. Here, we expect root damage to affect aboveground PRI because we assume that the efficiency of the leaves to assimilate carbon will be reduced following functional damage. Hence,

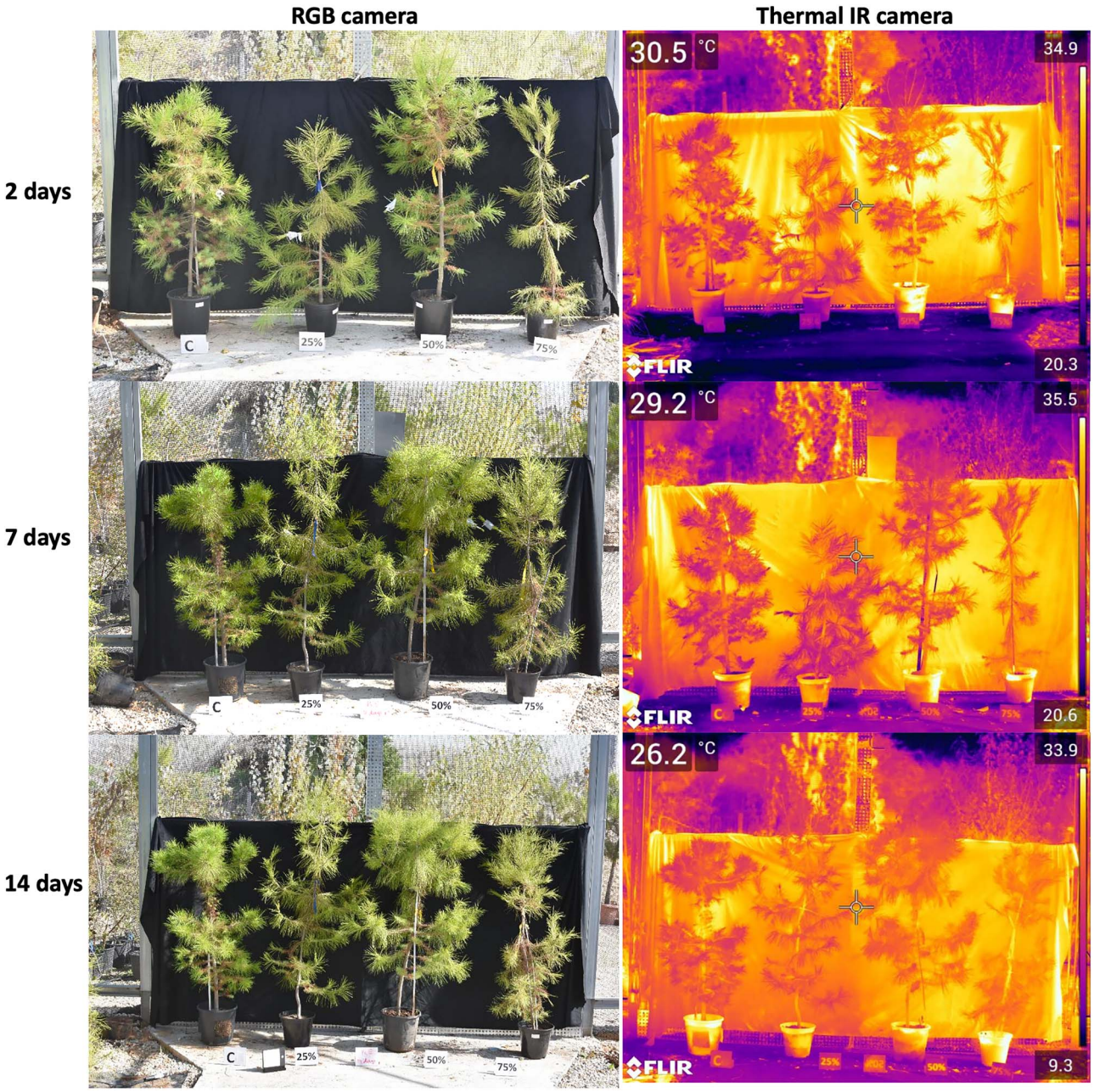

Figure 2 Phenotypic changes in *Pinus halepensis* saplings 2, 7 and 14 days following mechanical root damage (control and three levels: 25, 50 and 75 percent, left to right in each image). Note the different temperature ranges among the thermal images (top and bottom right corners in each of the three right panels). The white reference used to calibrate the image for light conditions is seen in the bottom left RGB image (14 days).

functional damage to the aboveground assimilation capacity will be reflected by a reduced PRI.

The sensitivity of carotenoid-based indices, like the SIPI, is closely related to that of PRI in terms of response to stress. This is due to the fact that carotenoids work as complementary light-absorbing pigments, which can dissipate the photodynamic effect directly and indirectly. While PRI specifically tracks changes in xanthophylls, a series of molecules framed within the carotenoids group, SIPI looks more at the ratio of the bulk carotenoid to chlorophyll content, which may make it a little bit less sensitive to small reactions occurring in response to stresses compared with PRI.

The chlorophyll photosynthesis index ($CI_{red\text{-}edge}$) was first developed to estimate the canopy chlorophyll content of anthocyanin-free leaves. Generally, $CI_{red\text{-}edge}$ can be used to assess the photosynthetic activity in plants. Its calculation is based on the red-edge band (705 nm), which is a reflecting switch between the effect of plant pigments and the canopy/leaf structure (Gitelson *et al.*, 2005, 2006). The effectiveness of this index is based on the sensitivity of the red-edge band, which

Table 1 Formulation of the five spectral vegetation indices used in this study

Index	Full name	Formulation	Reference
PRI	Photochemical reflectance index	$\frac{R_{531}-R_{570}}{R_{531}+R_{570}}$	Gamon *et al.*, 1992
$CI_{red\text{-}edge}$	Chlorophyll photosynthesis index	$\frac{R_{783}}{R_{705}}-1$	Gitelson *et al.*, 2005
NDWI	Normalized difference water index	$\frac{R_{550}-R_{790}}{R_{550}+R_{790}}$	McFeeters, 1996
ARI1	Anthocyanin reflectance index 1	$\frac{1}{R_{550}}-\frac{1}{R_{700}}$	Gitelson *et al.*, 2001
SIPI	Structure insensitive pigment index	$\frac{R_{800}-R_{445}}{R_{800}-R_{680}}$	Penuelas *et al.*, 1995

Note: $R_{\#}$ is the reflectance at wavelength #.

shows a relatively strong response to the changes in chlorophyll content, especially under stress conditions, shifting towards longer wavelengths with increased chlorophyll content or water content and towards shorter wavelengths with decreased chlorophyll or water content (Filella and Penuelas, 1994; Main *et al.*, 2011).

The ARI1 was formulated primarily based on the reflectance of anthocyanins. ARI1 is sensitive to anthocyanin accumulation in leaves, mainly through new growth and senescing leaves (Gitelson *et al.*, 2001; Oren-Shamir, 2009). When stress occurs, anthocyanin is usually accumulated to help with photoinhibition following disease, drought and physical damage in plants (Yu *et al.*, 2021). ARI1 should provide an early indication of plant damage (or other stress) via anthocyanin accumulation.

Finally, we use the NDWI to assess the long-term impact (on the scale of days) on the leaf water content. There are several versions of this index (Gao, 1996; McFeeters, 1996; Helman and Mussery, 2020). Here, we used the version based on the 550- and 790-nm bands (Table 1) because our hyperspectral data were confined to the VIS–NIR wavelength range (400–1000 nm). This version of NDWI provides negative values for materials containing water and positive values for completely dry materials. Thus, we expect desiccated leaves to be less negative or with smaller negative values than the hydrated leaves.

Statistical analyses

Data from all measurements were grouped by species, time of measurement (time after root damage (TARD)), root damage and measurement type. Statistical analyses were performed on each species and date separately through an analysis of variance (ANOVA) test followed by a Tukey HSD *post hoc* test for significant differences among root damage classes (0, 25, 50 and 75 percent) as well as via a three-way ANOVA test for the interaction Species × TARD × Root damage. The Shapiro–Wilk test was used to ensure a normal distribution of the data before conducting the ANOVA. Data that did not fulfil the normality assumption were transformed using the Normal Score Transformation method (Krzysztofowicz, 1997; Pyrcz and Deutsch, 2018). This method converts a data set so that it closely resembles a normal standard distribution curve by comparing the cumulative frequency value (y: 0–1) of the original data point (x) corresponding to the cumulative frequency *vs* a normal score of a typical normal distribution curve, point by point. The results from the ANOVA are summarized in Table 2, and all Tukey test results are marked directly on the boxplots in Figures 3–9. All statistical analyses were performed using the JMP 15 Pro statistical software (SAS Institute, Cary, NC, USA).

Results

Leaf greenness and temperature responses to root damage

Phenotypic differences among trees from different root damage groups, as detected by an RGB camera, were mild (Figure 1). Values of the green index ranged between 0.40–0.42 and decreased to as low as 0.30 after 30 days from root damage (i.e. in *Ceratonia*; Figure 2). Though the decrease was already observed after 4 days for saplings with 75 percent root damage, the difference from control saplings was statistically significant only after 30 days (Table 2). The only exception was *Pinus*, which did not display a significant difference from control even after 30 days following the damage.

In contrast to the green index, leaf temperature difference $\Delta T_{leaf\text{-}air}$, measured 3 h, 2 days and 25 days following root cutting, showed a significant difference from control saplings as early as 2 days following the root damage at both 50 percent and 75 percent root damage in *Ceratonia* and *Quercus* (Figures 3 and 4; Table 2). These changes were exacerbated at 25 days, when almost all damaged saplings (including the 25 percent root damage) had a greater $\Delta T_{leaf\text{-}air}$ than control saplings up to 3°C in *Ceratonia* and *Quercus* with a 75 percent root damage.

Vegetation indices response to root damage

PRI, a measure of the RUE (and indicative of photosynthesis), showed a significant decrease in two species already at day 4 (*Ceratonia* and *Pinus*; Figure 5). These responses were maintained on day 7 and mostly exacerbated on day 14, when PRI was significantly lower for all treated *Ceratonia* and *Quercus*, regardless of the level of damage, and for the 75 percent damaged *Pinus*. The $CI_{Red\text{-}edge}$ showed species-specific responses (Figure 6). There was no significant response in *Pinus*, a delayed response in *Quercus* and an early response in *Ceratonia*, affecting all treated saplings on days 7 and 14 following the root damage (Table 2). NDWI was also species-specific, with no significant *Pinus* response and a significant *Quercus* increase at day 14 (Figure 7; Table 2), likely indicating leaf desiccation. NDWI seemed to increase in *Ceratonia* already on day 4, but this increase was not significant even on

Table 2 Statistics *F* ratio and *P*-value > *F* ratio of full factorial three-way ANOVA for the sensing metrics PRI, $CI_{red\text{-}edge}$, NDWI, ARI1, SIPI, $\Delta T_{leaf\text{-}air}$ (°C) and greenness (GCC); the three factors are (1) species: *Pinus*, *Ceratonia* and *Quercus*; (2) root damage: 0, 25, 50 and 75 percent and (3) TARD, which corresponds to measurements done 4, 7 and 14 days after damage for PRI, $CI_{red\text{-}edge}$, NDWI, ARI1 and SIPI; 3 h, 2 days and 25 days for $\Delta T_{leaf\text{-}air}$; and 3 h, 4 days, 14 days and 30 days for greenness; statistically significant effects ($P < 0.05$) are marked in bold.

		PRI		Cl red-edge		NDWI		ARI1		SIPI	
Factor	*N*	*F* ratio	Prob > *F*	*F* ratio	Prob > *F*	*F* ratio	Prob > *F*	*F* ratio	Prob > *F*	*F* ratio	Prob > *F*
Species	2	39.82	**<0.0001**	115.64	**<0.0001**	185.96	**<0.0001**	156.78	**<0.0001**	4.20	**0.017**
TARD	2	2.78	0.07	0.57	0.57	0.09	0.91	6.45	**0.002**	4.66	**0.01**
TARD ∗ species	4	1.33	0.26	4.34	**0.0024**	6.03	**0.0002**	5.72	**0.0003**	11.70	**<0.0001**
Root damage	3	52.28	**<0.0001**	20.57	**<0.0001**	7.00	**0.0002**	12.50	**<0.0001**	24.36	**<0.0001**
Species ∗ root damage	6	7.11	**<0.0001**	3.75	**0.0017**	1.72	0.12	1.89	0.09	3.17	**0.006**
TARD ∗ root damage	6	1.60	0.15	0.88	0.51	1.04	0.41	1.38	0.23	0.86	0.53
Species ∗ TARD ∗ root damage	12	0.65	0.80	0.68	0.76	1.01	0.44	1.87	**0.04**	1.29	0.23

		$\Delta T_{leaf\text{-}air}$ (°C)			Greenness	
Factor	*N*	*F* Ratio	Prob > *F*	*N*	*F* ratio	Prob > *F*
Species	2	11.16	**<0.001**	2	4.19	**0.02**
TARD	2	36.57	**<0.001**	3	10.78	**<0.001**
Species × TARD	4	3.97	**<0.001**	6	4.47	**<0.001**
Root damage	3	28.85	**<0.001**	3	19.73	**<0.001**
Species × root damage	6	0.51	0.80	6	3.36	**0.004**
TARD × root damage	6	1.51	0.18	9	3.59	**<0.001**
Species × TARD × root damage	12	0.19	0.99	18	0.54	0.94

day 14. ARI1 increased after 14 days in *Ceratonia* and *Quercus* saplings with 75 percent root damage but did not change in *Pinus* (Figure 8). An early ARI1 increase, however, was observed in all treated *Quercus* saplings (25, 50 and 75 percent) after 4 days. Three days later, this apparent difference between the treated and control saplings disappeared (Figure 8). SIPI decreased in *Ceratonia* saplings with 75 percent root damage already after 4 days and in all three species after 7 days (Figure 9). Only in *Ceratonia,* there was a decrease in SIPI for saplings with 50 percent root damage (already after 7 days).

Discussion

We presented a first-of-its-kind experiment on aboveground responses to belowground damage in forest trees, taking advantage of the non-destructive optical and thermal methods. Overall, the aboveground response to root damage (1) was detected earlier in higher levels of root damage, and (2) the response became more noticeable with time. The first observation indicates an exposure-dependent response, which supports the notion that measured responses were directly linked to the root damage. The second observation suggests that aboveground responses to belowground damage were gradual and delayed. Repair and/or acclimation mechanisms, if any, were either faster than our observation intervals (e.g. in the case of *Pinus*, observing little responses), or, vice versa, insufficient in the long term, since damage increased with time. The latter is in agreement with previous studies showing a gradual decline in aboveground functions following trenching (Fini *et al*., 2013), root pruning (Schupp and Ferree, 1988, Benson *et al*., 2019), root reduction (Vitaly *et al*., 2019) or mature tree transplantation (Dror *et al*., 2020). We clarify that our findings cannot be reversed, i.e. responses detected aboveground are not necessarily exclusive to the belowground damage. Instead, they could reflect a myriad of aboveground responses to diverse abiotic and biotic stressors. For example, atmospheric drought, bark beetles and fire could also lead to canopy responses similar to those observed here. However, in cases where aboveground responses are detected, and no stressor is identified, our approach can provide good indications of involvement of belowground root damages.

Based on previous studies, we hypothesized that root damage would induce a fast reduction (hours to a few days) in tree water uptake (as in Dror *et al*., 2020), which will be expressed in leaf warming (Lapidot *et al*., 2019) and desiccation. While we confirmed the fast leaf warming responses (Figure 4), we did not observe a fast response in leaf desiccation, as NDWI changed very little (Figure 7). It is possible that the hardy leaf response is unique to our Mediterranean, drought-exposed tree species. However, an experiment in the dry season might have yielded larger responses and perhaps even mortality. Other limitations of our setup relate to the pots: they were too small to allow free root growth (see Materials and methods), root distribution in the pots was not entirely homogeneous (although quantified; see Materials and methods) and hence the treatments did not accurately represent the portions of root biomass removed. On the other hand, the fact that roots reached the bottom of pots supported our cutting approach as induction of root damage (Figure 1). This was true across the three species, which also had a similar tap root:lateral

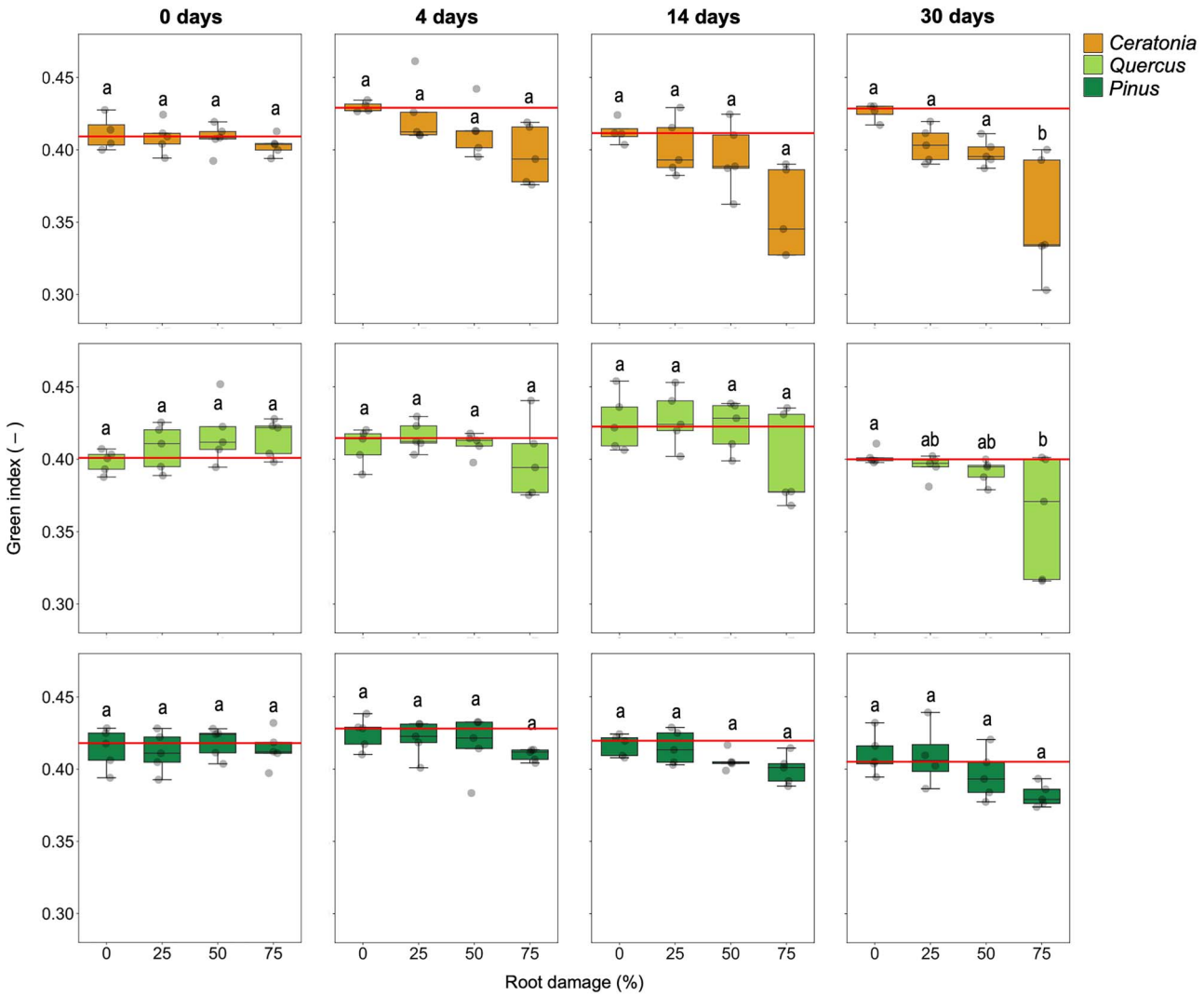

Figure 3 Dynamics of leaf greenness following mechanical root damage (three levels: 25, 50 and 75 percent, and control, 0 percent) in three Mediterranean forest tree species. Grey dots are the samples ($n = 5$ trees). Boxes indicate the first and third quartiles and the median of the five samples. Red horizontal lines denote the median value of the control for each species and time-point. Different letters indicate a significant difference among root damage levels per Tukey's HSD test at $P < 0.05$.

roots biomass ratio, avoiding any bias among species. In addition, our results pertain to saplings and not to mature trees, although similar responses have been detected among saplings and trees in a previous experiment with the same species (Lapidot *et al.*, 2019).

We next hypothesized that feedback on photosynthesis would follow (several days), eventually leading to a reduction in leaf greenness (days to weeks). Again, our hypothesis was only partly confirmed: leaf chlorophyll photosynthesis index and, more so, PRI showed significant reductions (Figures 5 and 6, respectively), yet leaf greenness was stable (Figure 3; except for 75 percent root damage after 30 days in two of the species). Last, we hypothesized that responses would appear at ≥50 percent damage, but not at 25 percent damage, owing to root redundancy. While this was true for *Pinus* in four out of the seven metrics, *Quercus* and *Ceratonia* showed root damage sensitivity even at 25 percent root damage in PRI and the other metrics (Figure 10).

The fundamental physiological questions posed here concern root system redundancy and the relative sensitivity of tree processes and functions to root damage. Simultaneously, we asked which non-destructive sensing metrics are the most sensitive to detect root damage, to what extent of damage and how fast. The two points of view are essentially two angles of the same object: the most sensitive measurement is also the one that relates to the plant function that is most affected by root damage. Similarly, changes in detection with time are the dynamics of the cascade of damage and recovery.

Among the seven sensing metrics, ΔT and PRI were the most sensitive, with ΔT responses as early as 2 days following root damage and PRI responses detectable even at 25 percent root

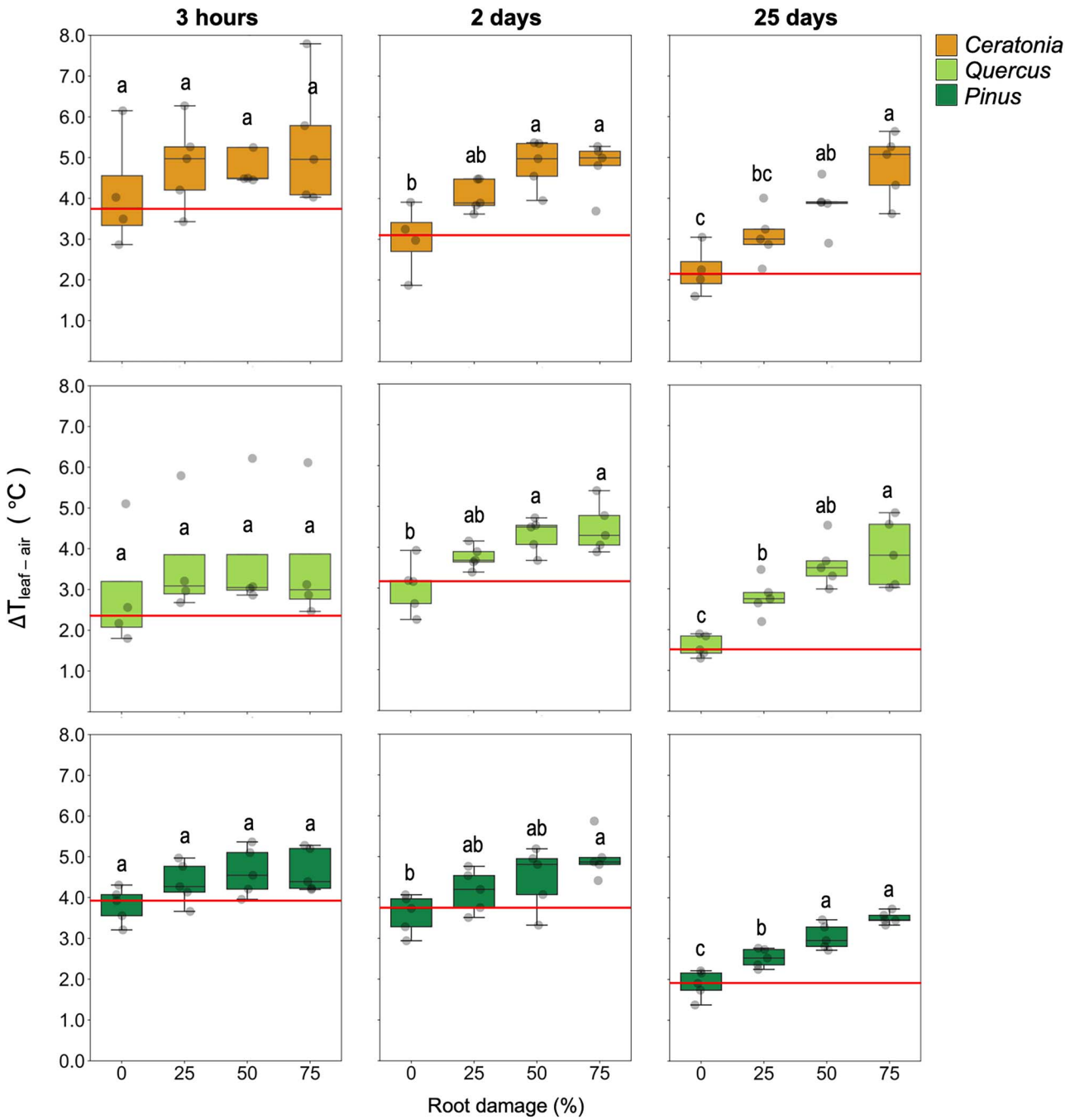

Figure 4 Dynamics of leaf-air temperature difference ($\Delta T_{leaf\text{-}air}$) following mechanical root damage (three levels: 25, 50 and 75 percent, and control, 0 percent) in three Mediterranean forest tree species. Grey dots are the samples ($n = 5$ trees). Boxes indicate the first and third quartiles and the median of the five samples. Red horizontal lines denote the median value of the control for each species and time-point. Different letters indicate a significant difference among root damage levels per Tukey's HSD test at $P < 0.05$.

damage after 14 days (Figure 10). This is in agreement with previous studies showing the utility of PRI (Suárez *et al.*, 2008; Panigada *et al.*, 2014; Helman and Mussery, 2020) and ΔT (Klapp *et al.*, 2021; Mulero *et al.*, 2022) in plant water stress detection. Our results align with earlier reports of photoinhibition and reduced transpiration following root damage (Fini *et al.*, 2013; Benson *et al.*, 2019). At the other end, NDWI and greenness were the least sensitive, with responses detectable only at 75 percent and as late as 14 or 30 days following root damage. Overall, the ΔT values measured here were similar to those measured with seedlings of the same species, showing 1–5°C, with extremes at up to 8°C (Lapidot *et al.*, 2019). Yet, we did not observe that ΔT increased from conifer needles to broadleaves and leaf size. Instead, ΔT was similar across species and diverged only with

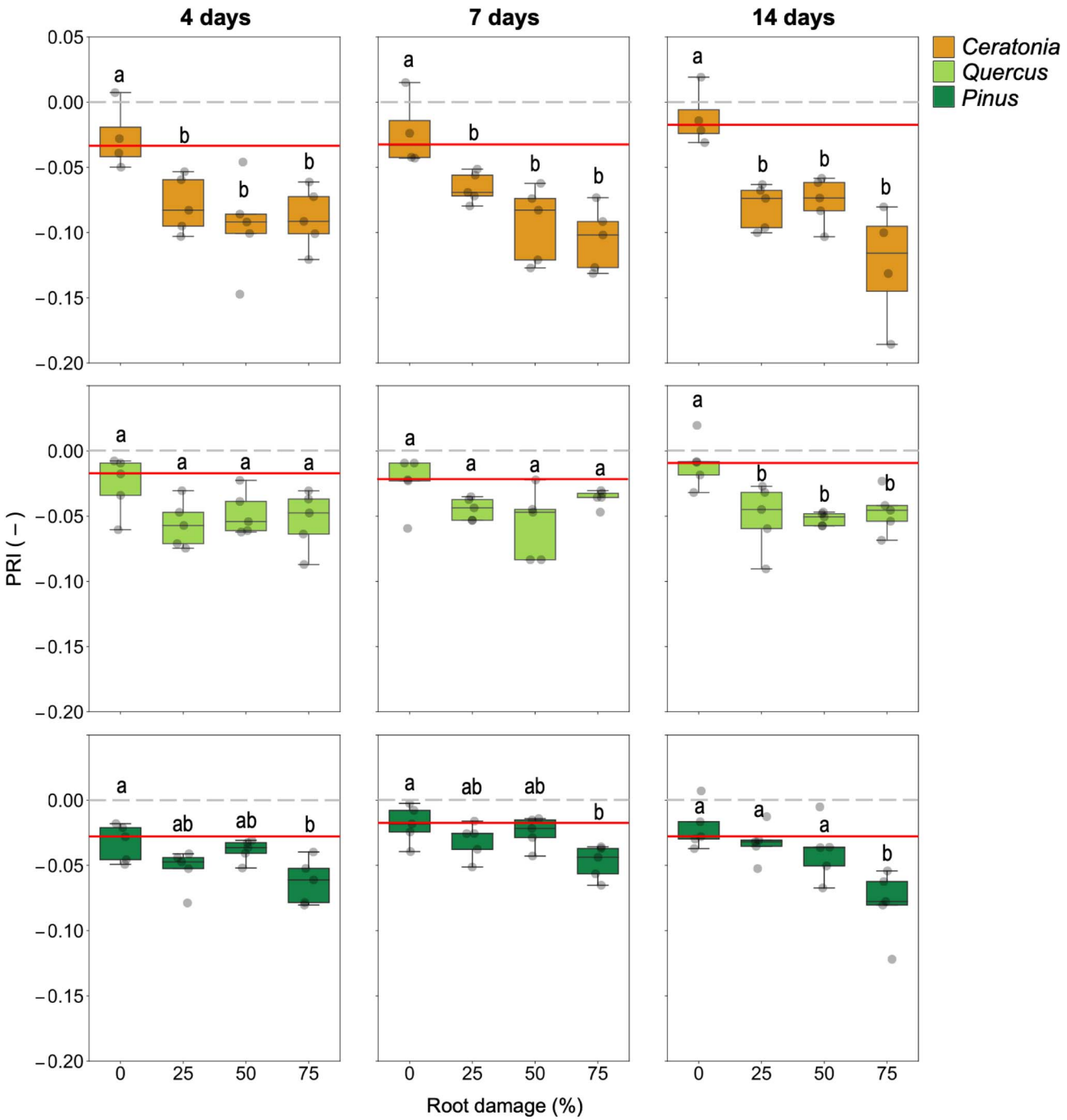

Figure 5 Dynamics of leaf Photochemical Reflectance Index (PRI) following mechanical root damage (three levels: 25, 50 and 75 percent, and control, 0 percent) in three Mediterranean forest tree species. Grey dots are the samples ($n = 5$ trees). Boxes indicate the first and third quartiles and the median of the five samples. Red horizontal lines denote the median value of the control for each species and time-point. Different letters indicate a significant difference among root damage levels per Tukey's HSD test at $P < 0.05$.

damage. This means that it might be possible to detect trees with root damage using thermal imaging across species.

Responses varied vastly among species, with *Ceratonia* being the most sensitive and *Pinus* being the least (Figure 10). The higher sensitivity of *Ceratonia* was expressed mainly in the response of PRI and $CI_{Red\text{-}edge}$ to root damage, which was detectable at 50 percent damage after just 4 days, and ARI1, which showed a clear response at 25 percent, only after 4 days. PRI and $CI_{Red\text{-}edge}$ responded even at 25 percent damage. *Pinus* was remarkably resistant to root damage, with PRI responses

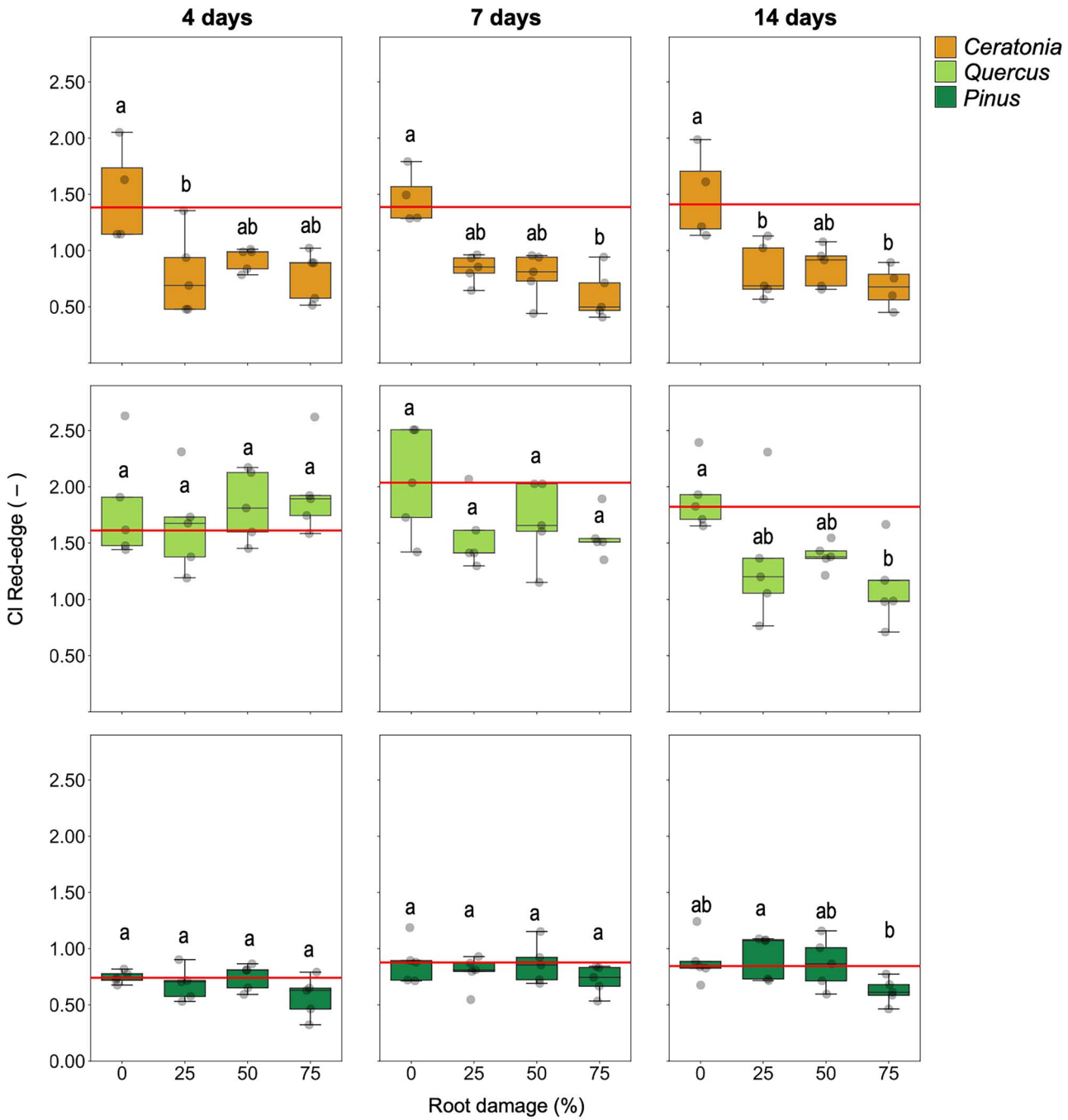

Figure 6 Dynamics of leaf chlorophyll photosynthesis index ($CI_{Red\text{-}edge}$) following mechanical root damage (three levels: 25, 50 and 75 percent, and control, 0 percent) in three Mediterranean forest tree species. Grey dots are the samples ($n = 5$ trees). Boxes indicate the first and third quartiles and the median of the five samples. Red horizontal lines denote the median value of the control for each species and time-point. Different letters indicate a significant difference among root damage levels per Tukey's HSD test at $P < 0.05$.

steadily shown only at 75 percent damage. Yet, even *Pinus* showed a clear response at 25 percent in ΔT at 25 days following damage. The responses of *Quercus* were typically higher than the responses of *Pinus* (and smaller than those of *Ceratonia*) and were usually delayed. An example of that was PRI of which no response was detected until 14 days following the damage. Here, *Ceratonia* had smaller root biomass than *Quercus* and *Pinus* (see Materials and methods). Among the three species, rooting depth in the field is greater in *Ceratonia* > *Quercus* > *Pinus* (Rog *et al.*, 2021). Our damage was applied from bottom to top, so higher sensitivity may relate to the lower root biomass or a potentially higher root fraction at depth. Another potential advantage for *Pinus* over the broadleaf species is in its xylem architecture: water is transported in *Pinus* through short tracheids

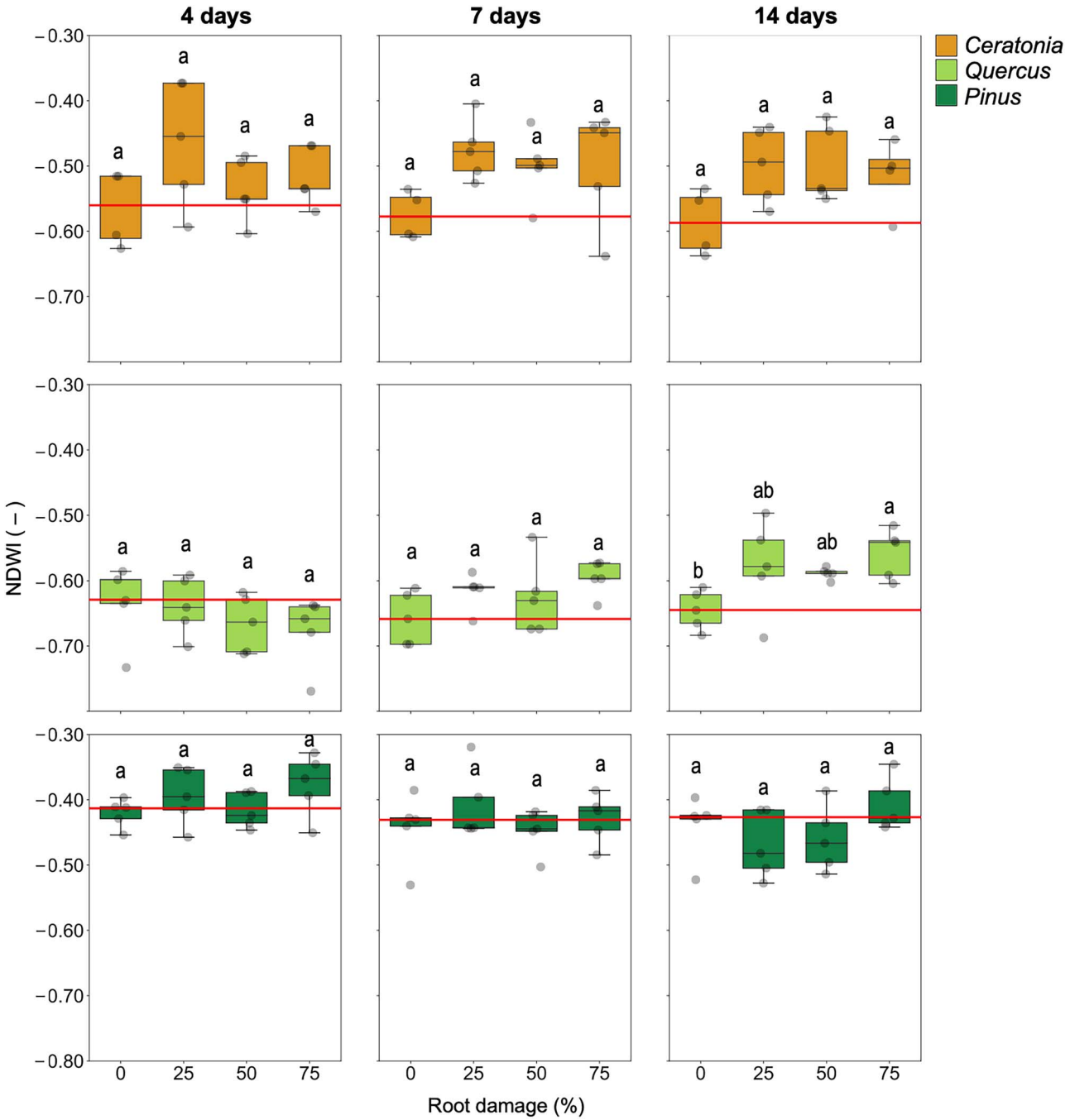

Figure 7 Dynamics of leaf Normalized Difference Water Index (NDWI) following mechanical root damage (three levels: 25, 50 and 75 percent, and control, 0 percent) in three Mediterranean forest tree species. Grey dots are the samples ($n = 5$ trees). Boxes indicate the first and third quartiles and the median of the five samples. Red horizontal lines denote the median value of the control for each species and time-point. Different letters indicate a significant difference among root damage levels per Tukey's HSD test at $P < 0.05$.

(David-Schwartz *et al.*, 2016), whereas in *Ceratonia* and *Quercus*, water is transported through long vessels (Cochard *et al.*, 2010). As a result, it is potentially easier for water to move both vertically and horizontally in *Pinus*, while in the broadleaf species, a single vessel might connect from root to leaf (a phenomenon termed hydraulic segmentation or sectorial flow). Hence, it is possible that water supply could be maintained despite root damage in *Pinus* but less so in the other species. Other drought resistance traits could also play a role, yet the three species co-habitat the semi-arid fringes of the Mediterranean.

The aboveground response of ΔT to belowground damage was straightforward compared with NDWI. ΔT is strongly related to the transpiration and water use (Lapidot *et al.*, 2019; Mulero *et al.*, 2022), whereby higher ΔT is associated with lower

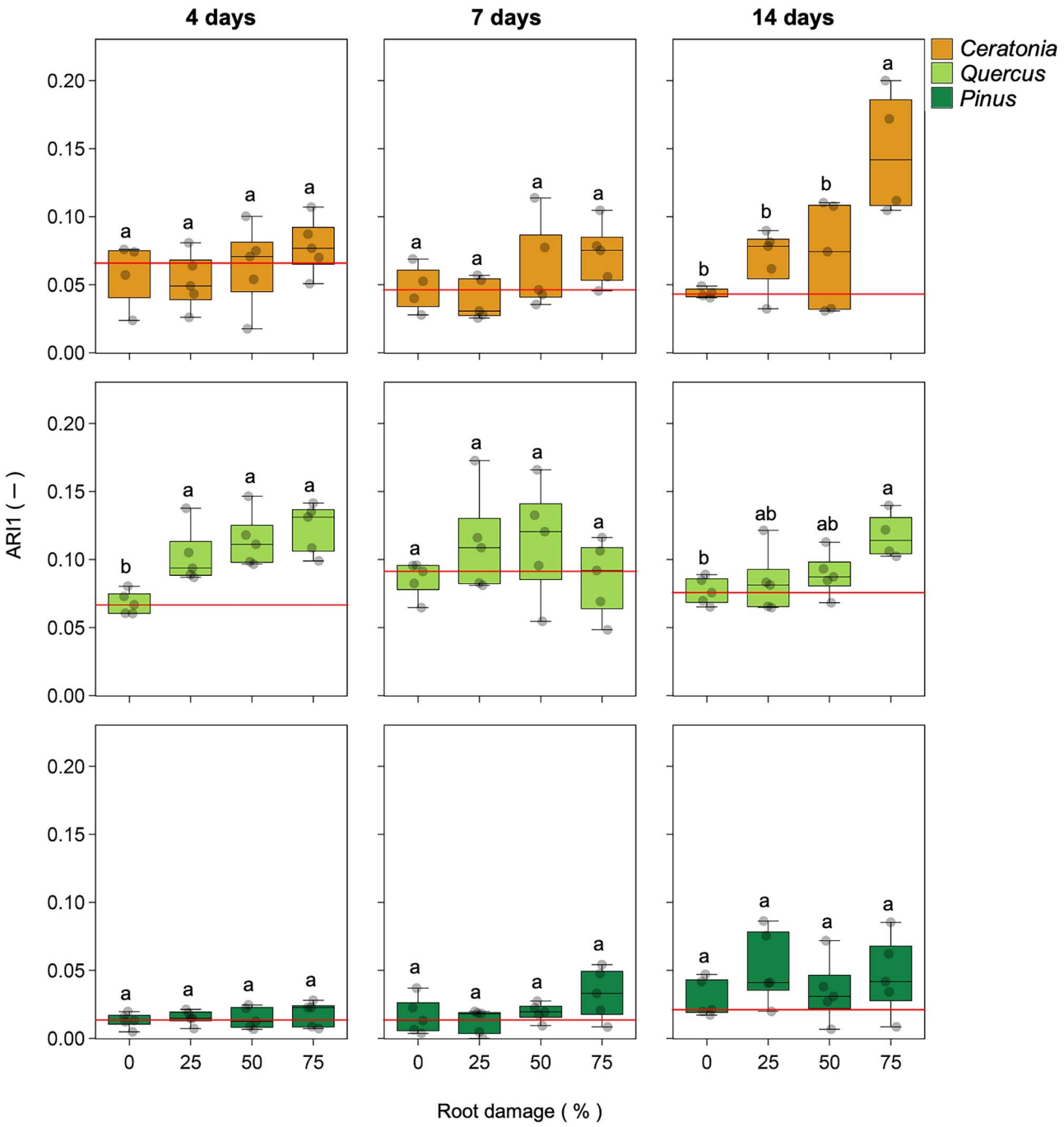

Figure 8 Dynamics of leaf Anthocyanin Reflectance Index 1 (ARI1) following mechanical root damage (three levels: 25, 50 and 75 percent, and control, 0 percent) in three Mediterranean forest tree species. Red horizontal lines denote the median value of the control for each species and time-point ($n = 5$ trees). Different letters indicate a significant difference among damage levels per Tukey's HSD test at $P < 0.05$.

transpiration rates. The lower transpiration of the damaged saplings even under watered conditions indicates functional stress; yet, it might also serve as an adaptive mechanism to prevent excessive water loss and a following leaf desiccation (Wuenscher and Kozlowski, 1971). This was likely the reason for the less noticeable, late increase in NDWI, pointing to some degree of leaf desiccation, mostly in *Quercus* and *Ceratonia*. The combination of ΔT and NDWI could serve to detect short-term water stress and, at the same time, long-term leaf desiccation.

PRI, SIPI and $CI_{Red\text{-}edge}$ are indicative of photosynthetic activity (Peñuelas *et al.*, 2011; Peng and Gitelson, 2012). Yet, there are specific differences between the response of these metrics to abiotic and biotic stresses (Nestola *et al.*, 2018). For example,

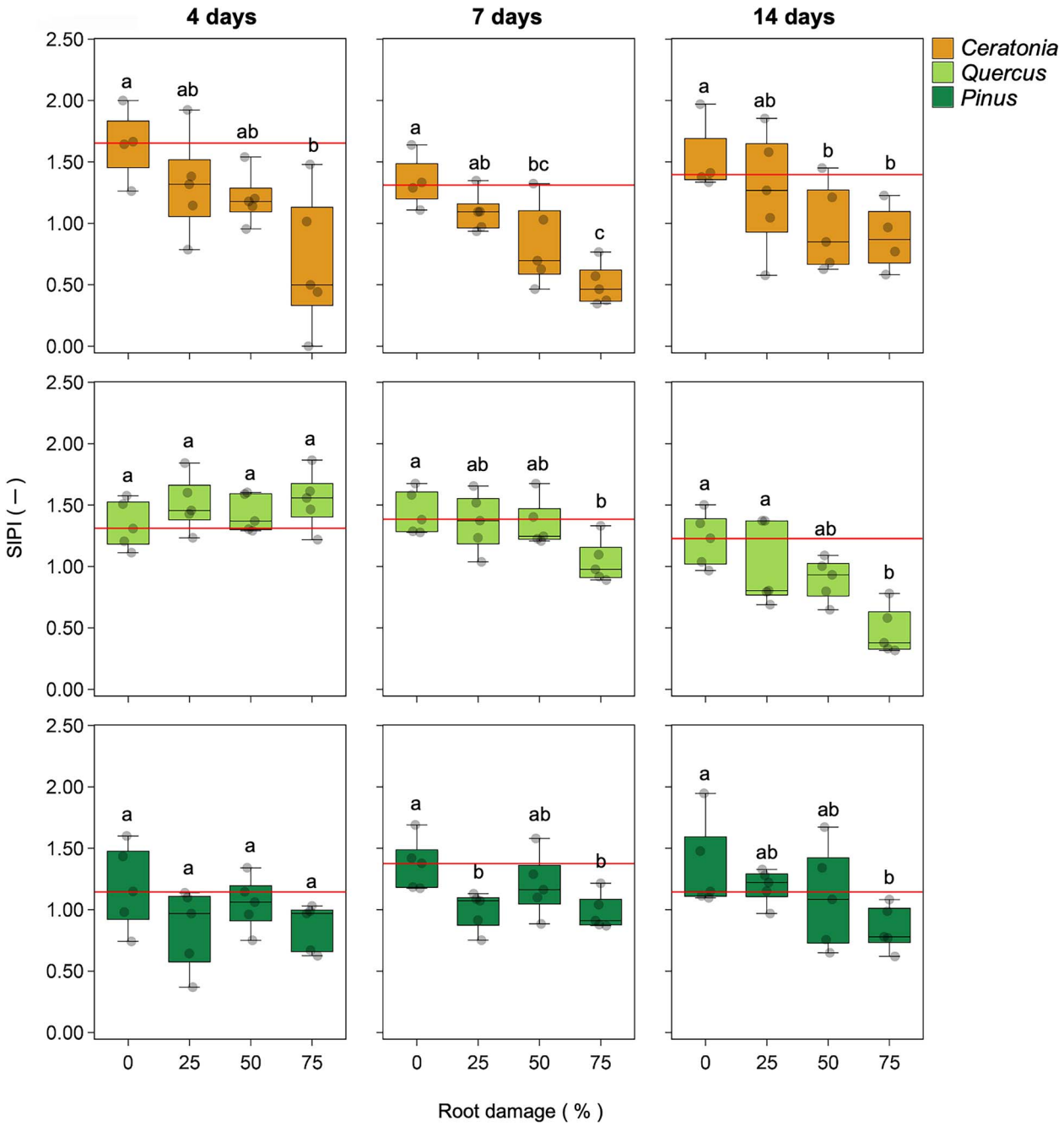

Figure 9 Dynamics of leaf Structure Insensitive Pigment Index (SIPI) following mechanical root damage (three levels: 25, 50 and 75 percent, and control, 0 percent) in three Mediterranean forest tree species. Red horizontal lines denote the median value of the control for each species and time-point ($n = 5$ trees). Different letters indicate a significant difference among damage levels per Tukey's HSD test at $P < 0.05$.

$CI_{Red\text{-}edge}$ has been shown to be a good proxy for chlorophyll content in chestnut, wild vine, beech trees and crops such as maize and wheat (Gitelson *et al.*, 2003; Peng and Gitelson, 2011; Walsh and Shafian, 2018). The ability of $CI_{Red\text{-}edge}$ to detect changes in the chlorophyll content is based on its dependence on the red-edge band, which is responsive to the chlorophyll pigment. However, because changes in the chlorophyll content in response to short-term stress may be slow (up to several days), $CI_{Red\text{-}edge}$ will often not detect such changes immediately (Nestola *et al.*, 2018). $CI_{Red\text{-}edge}$ tracks mainly canopy biochemical and structural attributes rather than directly photosynthesis rate. In that sense, PRI is more directly linked to photosynthesis through the xanthophyll cycle and can detect immediate damage to the photosynthetic apparatus (Merlier *et al.*, 2015). This was likely the reason for the early response in PRI and the late response in $CI_{Red\text{-}edge}$ observed in the treated saplings.

While PRI is specifically sensitive to xanthophyll changes, a series of molecules framed within the carotenoids group, SIPI

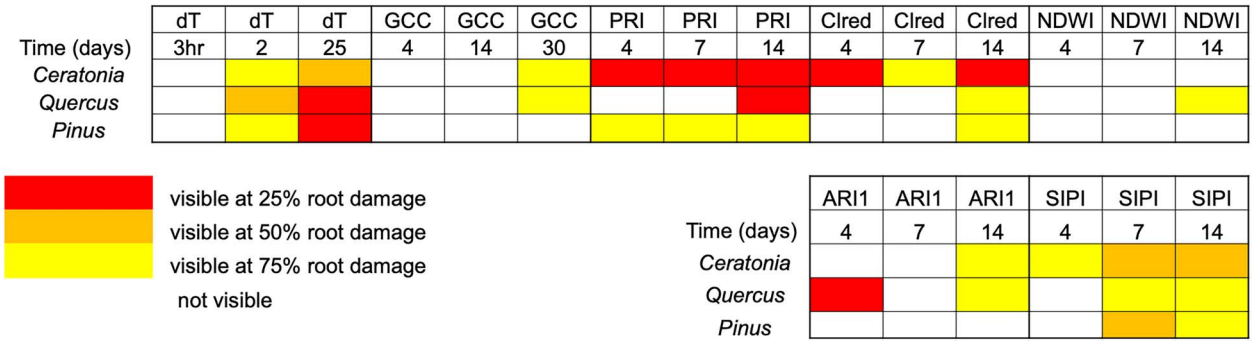

Figure 10 Visibility of aboveground responses as a function of belowground damage level in three Mediterranean forest tree species (rows) and across seven parameters at three time-points each (columns).

is more reflective of changes in the ratio of the bulk carotenoid to chlorophyll concentration. As such, SIPI is less sensitive to reactions occurring in response to light stress compared with PRI. This was manifested in our results through SIPI changes mostly at the extreme root damage (75 percent) and much less at low and moderate damage levels. ARI1, formulated primarily based on the reflectance of anthocyanins, is sensitive to anthocyanin accumulation in leaves via new growth and senescing leaves (Gitelson *et al.*, 2001; Oren-Shamir, 2009). In response to stress, anthocyanin is usually accumulated to help with photoinhibition following disease, drought and damage in plants (Yu *et al.*, 2021). The early response of ARI1 in all treated *Quercus* saplings suggests a fast anthocyanin accumulation in response to the root damage (fourth day for 25, 50 and 75 percent, as shown in Figure 8). Surprisingly, this was much less obvious in the *Ceratonia* and *Pinus* saplings. Moreover, the early increase in ARI1 was no longer apparent after 3 days (7 days after root damage) even in *Quercus*, suggesting a fast, yet, inconsistent anthocyanin response to root-damage stress.

The ability to track changes in the chlorophyll content in plants by remote sensing is also highly dependent on leaf characteristics such as leaf size, shape and age (Wilson and Cooper, 1969; Croft and Chen, 2018). For example, pines have been shown to have a much lower chlorophyll concentration than broadleaf trees, such as oaks, due to the long needle shape of their leaves (Li *et al.*, 2018). This difference in chlorophyll content is often expressed in spectral-based metrics, such as $CI_{Red\text{-}edge}$, which showed lower values in *Pinus* than in the broadleaves *Quercus* and *Ceratonia* species (Figure 6). Thus, changes in $CI_{Red\text{-}edge}$ due to stress (e.g. root damage, in our case) would be less detectable in *Pinus* than in *Quercus* and *Ceratonia*, possibly due to higher signal-to-noise ratio in the broadleaf species. By contrast, PRI, which is indicative of assimilation efficiency, would be more responsive to stress even in needleleaf species because of its higher sensitivity to small changes. Finally, since PRI is also indicative of photosynthesis (Garbulsky *et al.*, 2011), this gives it an advantage over other metrics, such as $CI_{Red\text{-}edge}$ and SIPI, in detecting aboveground responses to belowground damage.

Conclusions

This study demonstrates that root damage events in the pedosphere, which are not initially directly visible, can be visualized through indirect physiological responses with remote sensing. Tracking root damage from remote sensing platforms may contribute to our understanding of the physiological response related to root damage and also open avenues for mapping root damage events in time and space. Future research should, therefore, assess to what extent such remotely sensed metrics (e.g. vegetation indices) are sensitive to root damage in the presence of other stress events (e.g. droughts). Moreover, further experiments are necessary to test the sensitivity of optical remote sensing in real forest stands. We conclude that (1) although roots are redundant, mechanical damage will eventually decrease transpiration and photosynthesis across tree species. (2) In accordance with these physiological processes, leaf temperature and leaf PRI proved to be the most sensitive indices. (3) Abnormal leaf warming or reduced PRI might hence indicate root damage, e.g. following windstorm, drought, chemical or biotic attack or mechanical damage by the forest management activities.

Acknowledgements

We acknowledge the good collaboration of Itay Halevy, Nir Galili, Asaph Aharoni, Ilana Rogachev and Nir Shachaf (Weizmann Institute of Science). We thank Sophie Obersteiner (The Weizmann Tree Lab) for the design of Figure 1.

Conflict of interest statement

None declared.

Funding

Research was funded by an IMOD grant (Asaph Aharoni and T.K.). T. K. wishes to thank Yotam Project and Incumbent of the Edith and Nathan Goldenberg Career Development Chair.

Authors' contributions

M.A. performed the experiment following the research idea and guidance of T.K. M.A. measured and analysed the RGB and IR images. G.M. performed the spectral measurements and analyses under the mentorship of D.H. Y.O.-S. helped in the analysis of the measurements. D.H. and G.M. performed the statistical

analyses and created the graphs. T.K. wrote the paper with help from DH and all authors.

Data availability

All data used in this study are reported in the Results.

References

Abraham, J., Giacomuzzi, V. and Angeli, S. 2015 Root damage to apple plants by cockchafer larvae induces a change in volatile signals below-and above-ground. *Entomol. Exp. Appl.* **156**, 279–289. https://doi.org/10.1111/eea.12330.

Bardgett, R. D. (2018). Linking aboveground–belowground ecology: a short historical perspective. In *Aboveground–Belowground Community Ecology*. Springer, pp. 1–17. https://doi.org/10.1007/978-3-319-91614-9_1.

Benson, A.R., Morgenroth, J. and Koeser, A.K. 2019 The effects of root pruning on growth and physiology of two *Acer* species in New Zealand. *Urban For. Urban Green.* **38**, 64–73. https://doi.org/10.1016/j.ufug.2018.11.006.

Bezemer, T. M. and van Dam, N. M. 2005 Linking aboveground and belowground interactions via induced plant defenses. *Trends Ecol. Evol.*, **20**, 617–624, https://doi.org/10.1016/j.tree.2005.08.006.

Behmann, J., Acebron, K., Emin, D., Bennertz, S., Matsubara, S., Thomas, S. *et al.* 2018 Specim IQ: evaluation of a new, miniaturized handheld hyperspectral camera and its application for plant phenotyping and disease detection. *Sensors (Switzerland)* **18**, 441. https://doi.org/10.3390/s18020441.

Čermak, J., Jaroslav, S., Hana, K. and Soňa, T. 2013. Absorptive root areas of large pedunculate oak trees differing in health status along a road in South Bohemia, Czech Republic. *Urban forestry & urban greening*. **12**, 238–245.

Cochard, H., Herbette, S., Barigah, T., Badel, E., Ennajeh, M. and Vilagrosa, A. 2010. Does sample length influence the shape of xylem embolism vulnerability curves? A test with the Cavitron spinning technique. *Plant. Cell. Environ*. **33**(9), 1543–1552.

Croft, H., Chen, J.M. 2018 *Leaf Pigment Content, Comprehensive Remote Sensing*. Elsevier Inc. https://doi.org/10.1016/b978-0-12-409548-9.10547-0.

Crowther, T.W., Van den Hoogen, J., Wan, J., Mayes, M.A., Keiser, A.D., Mo, L. and Maynard, D. S. 2019. The global soil community and its influence on biogeochemistry. *Science*. **365**, eaav0550.

David-Schwartz, R., Paudel, I., Mizrachi, M., Delzon, S., Cochard, H., Lukyanov, V. *et al.* 2016. Indirect evidence for genetic differentiation in vulnerability to embolism in Pinus halepensis. *Front. Plant. Sci.* **7**, 768.

Demmig-Adams, B. and Adams III, W. W. 2006. Photoprotection in an ecological context: the remarkable complexity of thermal energy dissipation. *New. Phytol*. **172**(1), 11–21.

Dror, D., Weitzman, G., Rog, I., Kafri-Amit, T. and Klein, T. 2020. Physiological effects of mature tree transplanting characterize the roles of the soil-root interface in the field. *Agricultural and Forest Meteorology*. **295**, 108192.

Filella, I. and Penuelas, J. 1994 The red edge position and shape as indicators of plant chlorophyll content, biomass and hydric status. *Int. J. Remote Sens.* **15**, 1459–1470. https://doi.org/10.1080/01431169408954177.

Filella, I., Peñuelas, J., Llorens, L. and Estiarte, M. 2004 Reflectance assessment of seasonal and annual changes in biomass and CO2 uptake of a Mediterranean shrubland submitted to experimental warming and drought. *Remote Sens. Environ.* **90**, 308–318. https://doi.org/10.1016/j.rse.2004.01.010.

Fini, A., Frangi, P., Amoroso, G., Piatti, R., Robbiani, E., Sani, L. and Ferrini, F. 2013. Effects of root severance by excavation on growth, physiology and stability of two urban tree species: results from a long-term experiment. *Acta. Horticulturae*. **990**, 487–494.

Gamon, J.A., Kitajima, K., Mulkey, S.S., Serrano, L. and Wright, S.J. 2005 Diverse optical and photosynthetic properties in a neotropical dry forest during the dry season: implications for remote estimation of photosynthesis. *Biotropica* **37**, 547–560. https://doi.org/10.1111/j.1744-7429.2005.00072.x.

Gamon, J.A., Penuelas, J. and Field, C.B. 1992 A narrow-waveband spectral index that tracks diurnal changes in photosynthetic efficiency. **41**, 35–44. https://doi.org/10.1088/0305-4470/24/13/001.

Gamon, J.A., Serrano, L. and Surfus, J.S. 1997 The photochemical reflectance index: an optical indicator of photosynthetic radiation use efficiency across species, functional types, and nutrient levels. *Oecologia* **112**, 492–501. https://doi.org/10.1007/s004420050337.

Gao, B. 1996 NDWI—a normalized difference water index for remote sensing of vegetation liquid water from space. *Remote Sens. Environ.* **58**, 257–266. https://doi.org/10.1016/S0034-4257(96)00067-3.

Garbulsky, M.F., Peñuelas, J., Gamon, J., Inoue, Y. and Filella, I. 2011 The photochemical reflectance index (PRI) and the remote sensing of leaf, canopy and ecosystem radiation use efficiencies: a review and meta-analysis. *Remote Sens. Environ.* **115**, 281–297. https://doi.org/10.1016/j.rse.2010.08.023.

Gitelson, A.A., Gritz, Y. and Merzlyak, M.N. 2003 Relationships between leaf chlorophyll content and spectral reflectance and algorithms for non-destructive chlorophyll assessment in higher plant leaves. *J. Plant Physiol.* **160**, 271–282. https://doi.org/10.1078/0176-1617-00887.

Gitelson, A.A., Keydan, G.P. and Merzlyak, M.N. 2006 Three-band model for noninvasive estimation of chlorophyll, carotenoids, and anthocyanin contents in higher plant leaves. *Geophys. Res. Lett.* **33**, 1–5. https://doi.org/10.1029/2006GL026457.

Gitelson, A.A., Merzlyak, M.N. and Chivkunova, O.B. 2001 Optical properties and nondestructive estimation of anthocyanin content in plant leaves¶. *Photochem. Photobiol.* **74**, 38–45. https://doi.org/10.1562/0031-8655(2001)074<0038:opaneo>2.0.co;2.

Gitelson, A.A., Viña, A., Ciganda, V., Rundquist, D.C. and Arkebauer, T.J. 2005 Remote estimation of canopy chlorophyll content in crops. *Geophys. Res. Lett.* **32**, 1–4. https://doi.org/10.1029/2005GL022688.

Guariguata, M.R. 1998. Response of forest tree saplings to experimental mechanical damage in lowland Panama. *For. Ecol. Manag.* **102**, 103–111.

Helman, D., Lensky, I.M., Yakir, D. and Osem, Y. 2017a Forests growing under dry conditions have higher hydrological resilience to drought than do more humid forests. *Glob. Chang. Biol.* **23**, 2801–2817. https://doi.org/10.1111/gcb.13551.

Helman, D. and Mussery, A. 2020 Using Landsat satellites to assess the impact of check dams built across erosive gullies on vegetation rehabilitation. *Sci. Total Environ.* **730**, 138873. https://doi.org/10.1016/j.scitotenv.2020.138873.

Helman, D., Osem, Y., Yakir, D. and Lensky, I.M. 2017b Relationships between climate, topography, water use and productivity in two key Mediterranean forest types with different water-use strategies. *Agric. For. Meteorol.* **232**, 319–330. https://doi.org/10.1016/j.agrformet.2016.08.018.

Idso, S.B., Jackson, R.D., Ehrler, W.L. and Mitchell, S.T. 1969 A method for determination of infrared emittance of leaves. *Ecology*. **50**, 899–902.

Klapp, I., Yafin, P., Oz, N., Brand, O., Bahat, I., Goldshtein, E. *et al.* 2021. Computational end-to-end and super-resolution methods to

improve thermal infrared remote sensing for agriculture. *Precis. Agric.* **22**, 452–474.

Klein, T., Randin, C. and Körner, C. 2015. Water availability predicts forest canopy height at the global scale. *Ecol. Lett.* **18**, 1311–1320.

Kohzuma, K., Tamaki, M. and Hikosaka, K. 2021. Corrected photochemical reflectance index (PRI) is an effective tool for detecting environmental stresses in agricultural crops under light conditions. *J. Plant. Res.* **134**, 683–694.

Konopka B, Lukac M 2010, Fine root condition relates tovisible crown damage in Norway spruce in acidified soils. *For. Pathol.* **40**, 47–57.

Kováč, D., Veselovská, P., Klem, K., Večeřová, K., Ač, A., Peñuelas, J. *et al.* 2018 Potential of photochemical reflectance index for indicating photochemistry and light use efficiency in leaves of European beech and Norway spruce trees. *Remote Sens.* **10**, 1202. https://doi.org/10.3390/rs10081202.

Krzysztofowicz, R. 1997 Transformation and normalization of variates with specified distributions. *J. Hydrol.* **197**, 286–292.

Lapidot, O., Ignat, T., Rud, R., Rog, I., Alchanatis, V. and Klein, T. 2019 Use of thermal imaging to detect evaporative cooling in coniferous and broadleaved tree species of the Mediterranean maquis. *Agric. For. Meteorol.* **271**, 285–294. https://doi.org/10.1016/j.agrformet.2019.02.014.

Li, Y., He, N., Hou, J., Xu, L., Liu, C., Zhang, J. *et al.* 2018 Factors influencing leaf chlorophyll content in natural forests at the biome scale. *Front. Ecol. Evol.* **6**, 1–10. https://doi.org/10.3389/fevo.2018.00064.

Ma, S.C., Wang, T.C., Guan, X.K. and Zhang, X. 2018. Effect of sowing time and seeding rate on yield components and water use efficiency of winter wheat by regulating the growth redundancy and physiological traits of root and shoot. *Field Crops Res.* **221**, 166–174.

Main, R., Cho, M.A., Mathieu, R., O'Kennedy, M.M., Ramoelo, A. and Koch, S. 2011 An investigation into robust spectral indices for leaf chlorophyll estimation. *ISPRS J. Photogramm. Remote Sens.* **66**, 751–761. https://doi.org/10.1016/j.isprsjprs.2011.08.001.

McFeeters, S.K. 1996 The use of the normalized difference water index (NDWI) in the delineation of open water features. *Int. J. Remote Sens.* **17**, 1425–1432. https://doi.org/10.1080/01431169608948714.

Merlier, E., Hmimina, G., Dufrêne, E. and Soudani, K. 2015 Explaining the variability of the photochemical reflectance index (PRI) at the canopy-scale: disentangling the effects of phenological and physiological changes. *J. Photochem. Photobiol. B Biol.* **151**, 161–171. https://doi.org/10.1016/j.jphotobiol.2015.08.006.

Monteith, J.L. 1977 Climate and the efficiency of crop production in Britain. *Philos. Trans. R. Soc. Lond. Ser. B Biol. Sci.* **281**, 277–294. https://doi.org/10.1098/rstb.1977.0140.

Mulero, G., Jiang, D., Bonfil, D.J. and Helman, D. 2022 Use of thermal imaging and the photochemical reflectance index (PRI) to detect wheat response to elevated CO2 and drought. *Plant Cell Environ.* **46**, 76–92. https://doi.org/10.1111/pce.14472.

Nestola, E., Scartazza, A., Di Baccio, D., Castagna, A., Ranieri, A., Cammarano, M. *et al.* 2018 Are optical indices good proxies of seasonal changes in carbon fluxes and stress-related physiological status in a beech forest? *Sci. Total Environ.* **612**, 1030–1041. https://doi.org/10.1016/j.scitotenv.2017.08.167.

Oren-Shamir, M. 2009 Does anthocyanin degradation play a significant role in determining pigment concentration in plants? *Plant Sci.* **177**, 310–316. https://doi.org/10.1016/j.plantsci.2009.06.015.

Panigada, C., Rossini, M., Meroni, M., Cilia, C., Busetto, L., Amaducci, S. *et al.* 2014. Fluorescence, PRI and canopy temperature for water stress detection in cereal crops. *Int. J. Appl. Earth. Obs. Geoinf.* **30**, 167–178.

Peng, Y. and Gitelson, A.A. 2012 Remote estimation of gross primary productivity in soybean and maize based on total crop chlorophyll content. *Remote Sens. Environ.* **117**, 440–448. https://doi.org/10.1016/j.rse.2011.10.021.

Peng, Y. and Gitelson, A.A. 2011 Application of chlorophyll-related vegetation indices for remote estimation of maize productivity. *Agric. For. Meteorol.* **151**, 1267–1276. https://doi.org/10.1016/j.agrformet.2011.05.005.

Penuelas, J., Baret, F. and Filella, I. 1995 Semi-empirical indices to assess carotenoids/chlorophyll a ratio from leaf spectral reflectance. *Photosynthetica* **31**, 221–230.

Peñuelas, J., Garbulsky, M.F. and Filella, I. 2011 Photochemical reflectance index (PRI) and remote sensing of plant CO2 uptake. *New Phytol.* **191**, 596–599. https://doi.org/10.1111/j.1469-8137.2011.03791.x.

Porcar-Castell, A., Garcia-Plazaola, J.I., Nichol, C.J., Kolari, P., Olascoaga, B., Kuusinen, N. *et al.* 2012 Physiology of the seasonal relationship between the photochemical reflectance index and photosynthetic light use efficiency. *Oecologia* **170**, 313–323. https://doi.org/10.1007/s00442-012-2317-9.

Pyrcz, M.J. and Deutsch, C.V. 2018 *Transforming Data to a Gaussian Distribution*, Geostatistics Lessons, pp. 1–4.

Rog, I., Tague, C., Jakoby, G., Megidish, S., Yaakobi, A., Wagner, Y. and Klein, T. 2021. Interspecific soil water partitioning as a driver of increased-productivity in a diverse mixed Mediterranean forest. *J. Geophys. Res. Biogeosci.* **126**, e2021JG006382.

Sachs, T., Novoplansky, A. and Cohen, D. 1993. Plants as competing populations of redundant organs. *Plant Cell Environ.* **16**, 765–770.

Schindelin, J., Arganda-Carreras, I., Frise, E., Kaynig, V., Longair, M., Pietzsch, T. *et al.* 2012. Fiji: an open-source platform for biological-image analysis. *Nat. Methods.* **9**, 676–682.

Schupp, J.R., and Ferree, D.C. 1988. Root pruning for growth control in apple trees. In *IV International Symposium on Research and Development on Orchard and Plantation Systems* **243**, 103–110.

Suárez, L., Zarco-Tejada, P.J., Sepulcre-Cantó, G., Pérez-Priego, O., Miller, J.R., Jiménez-Muñoz, J.C. *et al.* 2008. Assessing canopy PRI for water stress detection with diurnal airborne imagery. *Remote Sens. Environ.* **112**, 560–575.

Sukhov, V., Sukhova, E., Khlopkov, A., Yudina, L., Ryabkova, A., Telnykh, A. *et al.* 2021 *Proximal Imaging of Changes in Photochemical Reflectance Index in Leaves Based on Using Pulses of Green-Yellow Light*. Remote Sensing, **13**. https://doi.org/10.3390/rs13091762.

Vitali, V., Ramirez, J.A., Perrette, G., Delagrange, S., Paquette, A. and Messier, C. 2019. Complex above-and below-ground growth responses of two urban tree species following root, stem, and foliage damage—an experimental approach. *Front. Plant. Sci.* **10**, 1100.

Walsh, S.O. and Shafian, S. 2018 *Assessment of Red-Edge Based Vegetation Indices Derived from Unmanned Arial Vehicle for Plant Nitrogen Content Estimation*. In *Proceedings of the 14th International Conference on Precision Agriculture*, Montreal, QC, Canada (pp. 24–27).

Wilson, D. and Cooper, J.P. 1969 Apparent photosynthesis and leaf characters in relation to leaf position and age, among contrasting Lolium genotypes. *New Phytol.* **68**, 645–655. https://doi.org/10.1111/j.1469-8137.1969.tb06468.x.

Winters, G., Otieno, D., Cohen, S., Bogner, C., Ragowloski, G., Paudel, I. *et al.* 2018. Tree growth and water-use in hyper-arid Acacia occurs during the hottest and driest season. *Oecologia*. **188**, 695–705.

Wuenscher, J.E. and Kozlowski, T.T. 1971 The response of transpiration resistance to leaf temperature as a desiccation resistance mechanism in tree seedlings. *Physiol. Plant.* **24**, 254–259. https://doi.org/10.1111/j.1399-3054.1971.tb03488.x.

Yu, Z.C., Lin, W., Zheng, X.T., Chow, W.S., Luo, Y.N., Cai, M.L. *et al.* 2021 The relationship between anthocyanin accumulation and photoprotection in young leaves of two dominant tree species in

subtropical forests in different seasons. *Photosynth. Res.* **149**, 41–55. https://doi.org/10.1007/s11120-020-00781-4.

Zhang, C., Filella, I., Liu, D., Ogaya, R., Llusià, J., Asensio, D. *et al.* 2017 Photochemical reflectance index (PRI) for detecting responses of diurnal and seasonal photosynthetic activity to experimental drought and warming in a Mediterranean shrubland. *Remote Sens.* **9**, 1–21. https://doi.org/10.3390/rs9111189.

Zhang, R. and Zhang, D. Y. 2000. A comparative study on root redundancy in spring wheat varieties released in different years in semi-arid areas. *Chin. J. Plant Ecol.* **24**, 298.